Medical Research Archives

European Society of Medicine

Published: January 31, 2024

Citation: Eaton L, Bengtsson J, et al., 2024. Sources of Reactive Oxygen Species in Normoxic and Hypoxic Naked Mole-Rat Brain, Medical Research Archives, [online] 12(1). https://doi.org/10.18103/mra.v12i1.4857

DOI
https://doi.org/10.18103/mra.v12i1.4857

ISSN: 2375-1924

RESEARCH ARTICLE

Sources of Reactive Oxygen Species in Normoxic and Hypoxic Naked Mole-Rat Brain

Liam Eaton[1], John Bengtsson[1], Isabella Welch[1], Abdul K. Halal[1], Matthew E. Pamenter[1,2,*]

[1]Department of Biology, University of Ottawa, Ottawa, ON, Canada
[2]University of Ottawa Brain and Mind Research Institute, Ottawa, ON, Canada

***Corresponding author:** mpamenter@uottawa.ca

Abstract
Oxygen availability dictates the rate of reactive oxygen species production from various cellular sources; excessive ROS accumulation can be cytotoxic. Mitochondria are usually the primary contributors to basal reactive oxygen species generation in the brain; however, xanthine oxidoreductase and nicotinamide adenine dinucleotide phosphate oxidase can also produce considerable reactive oxygen species during hypoxia/reoxygenation. In the brains of most mammals, cellular death accompanies hypoxia-mediated surges in reactive oxygen species production, but this is avoided in the cortex of hypoxia-tolerant naked mole-rats (*Heterocephalus glaber*). However, the contributions of various reactive oxygen species generators towards total reactive oxygen species homeostasis in naked mole-rat brain is unknown. We hypothesized that mitochondria remain the primary reactive oxygen species generators in naked mole-rat cortex and predicted that pharmacological inhibition of mitochondrial complex I would induce greater fluctuations in superoxide ($O_2^{\bullet-}$) and hydrogen peroxide (H_2O_2) than inhibition of xanthine oxidoreductase or nicotinamide adenine dinucleotide phosphate oxidase. To test this, we used fluorescence microscopy to measure H_2O_2 and $O_2^{\bullet-}$ production from cortical slices during normoxia and hypoxia while pharmacologically inhibiting mitochondrial complex I, xanthine oxidoreductase, or nicotinamide adenine dinucleotide phosphate oxidase. Unexpectedly, we found xanthine oxidoreductase inhibition induced the greatest increase in $O_2^{\bullet-}$ during normoxia and hypoxia (~100% and 70%, respectively). Hypoxic inhibition of nicotinamide adenine dinucleotide phosphate oxidase induced the greatest decrease in H_2O_2 by ~35% below baseline. Finally, although inhibition of mitochondrial complex I during hypoxia yielded significant fluctuations in $O_2^{\bullet-}$ and H_2O_2, these changes were considerably smaller than fluctuations induced by inhibiting xanthine oxidoreductase or nicotinamide adenine dinucleotide phosphate oxidase. Together, and unlike in other rodent brain, our results suggest that xanthine oxidoreductase is the primary contributor to reactive oxygen species production in naked mole-rat cortex.

Keywords: NADPH oxidase; mitochondria; electron transport system; xanthine oxidoreductase; superoxide; hydrogen peroxide; reactive oxygen species; hypoxia

Abbreviations:

ACSF – artificial cerebral spinal fluid
CM-H_2DCFDA – 5-(and-6)-chloromethyl-2',7'-dichlorodihydrofluorescein diacetate, acetyl ester
DHE – dihydroethidium
DPI – diphenyleneiodonium
ETS – electron transport system
H_2O_2 – hydrogen peroxide
NADPH – reduced nicotinamide adenine dinucleotide phosphate
NMDG – *N*-Methyl-D-Glucamine
NOX – NADPH oxidase
$O_2^{\bullet-}$ – superoxide
ROS – reactive oxygen species
XOR – xanthine oxidoreductase

Introduction

Reactive oxygen species (ROS) are potent second messengers that regulate a myriad of cellular components and processes[1-5]. As such, the production and scavenging of ROS are carefully balanced in healthy biological systems[6-8]. However, surges in ROS may occur during periods of environmental or tissues-level hypoxia and/or following reoxygenation, and are potentially induced by environmental oxygen availability, exhaustive exercise, or due to various pathophysiologies[9-11]. Increased production of ROS, whether in the form of superoxide anions ($O_2^{\bullet-}$) or hydrogen peroxide (H_2O_2), can deleteriously impact cellular function, promote apoptotic cell death[12], and/or cause oxidative damage to proteins, DNA, or lipids[6,13,14].

There are numerous sources of ROS in a cell and each of these systems have been linked to perturbations in ROS homeostasis during hypoxia and reoxygenation. In brain cells (and most other cell types), the primary source of ROS generation is the mitochondrial electron transport system (ETS). Depending on the species, it is estimated that 0.25-11% of all oxygen consumed for the process of oxidative phosphorylation leaks out of the ETS to form $O_2^{\bullet-}$ as a by-product of aerobic metabolism[15-18]. Intuitively, we might predict that ROS generation would decrease with less oxygen available (i.e., during hypoxia or ischemia); however, the concentration of electron donors within the mitochondrial ETS also rises during hypoxia, leading to increased ROS production relative to normoxia[19]. Sustained hypoxia ultimately leads to the slowing, and potentially reversal, of electron flow along the mitochondrial ETS, resulting in elevated ROS production and succinate accumulation[9,20-23]. Upon re-oxygenation, the accumulated succinate is rapidly oxidized, which results in a large spike in ROS production through complex I[24-26].

In addition to the mitochondrial ETS, xanthine oxidoreductase (XOR) and nicotinamide adenine dinucleotide phosphate (NADPH) oxidase (NOX) also contribute significantly to cellular ROS generation[27-30]. XOR is a cytosolic enzyme that is primarily involved in purine catabolism and produces ROS as a by-product of this reaction at relatively low levels compared to other major ROS generators[31]. As such, XOR is not often thought to substantially contribute to total cellular ROS production during normoxia[29,32]. However, during hypoxia, XOR activity increases in the rat adrenal medulla[29,33], and XOR-derived $O_2^{\bullet-}$ production spikes in cultured rat hippocampal neurons following exposure to oxygen glucose deprivation (OGD; a common in vitro ischemic treatment) and during chemically-induced anoxia with cyanide (NaCN; a common in vitro mimic of anoxia)[34]. Similarly, NOX is not usually a major contributor towards total normoxic ROS generation unless otherwise recruited as part of an immune response[35,36]. However, alongside cytochrome p450, NOX generates high levels of ROS within the endoplasmic reticulum as a by-product of protein folding and steroid biosynthesis[37,38], and a NOX-mediated ROS burst has also been reported in ischemic rat neurons[34].

Notably, all of the aforementioned studies were conducted in hypoxia-intolerant species. Conversely, studies from hypoxia-tolerant species, which experience periods of hypoxia in their natural environmental niche, suggest that such species avoid deleterious changes in ROS production during *in vitro* hypoxia or ischemia[39-43]. In these species, ROS homeostasis is largely maintained during hypoxia and reoxygenation. The mechanisms underlying this ability are poorly understood but likely involve a combination of preventing deleterious bursts of ROS generation from various cellular ROS sources, and/or enhancing ROS scavenging pathways[39,44-50]. Together, these strategies presumably prevent subsequent oxidative damage, which is likely beneficial in species which experience frequent hypoxic and normoxic transitions[44].

One hypoxia-tolerant species of interest is the eusocial and fossorial naked mole-rat (*Heterocephalus glaber*), which lives in intermittent hypoxia whilst underground[51,52]. Presumably because of this species' life history, naked mole-rats have evolved a wide variety of mechanisms to tolerate periods of hypoxia and reoxygenation[51], and are considered one of the most hypoxia-tolerant mammals studied to date. Previously, we reported that naked mole-rat cortex maintains ROS homeostasis during periods of *in vitro* hypoxia or ischemia, and during subsequent reoxygenation; whereas similarly treated mouse cortex exhibits large fluctuations in ROS and also nitric oxide[40,53,54]. In addition, naked mole-rat brain (and other tissues) avoid redox damage during periods of *in vivo* hypoxia[55]. This remarkable ability to maintain ROS homeostasis is due in part to a heightened ROS scavenging capacity in at least some tissues, as the glutathione (GSH) and thioredoxin (Trx) dependent ROS scavenging systems in naked mole-rat skeletal and cardiac muscle mitochondria are upregulated and can detoxify greater quantities of ROS than matched mouse tissues[45]. Presumably, similar robust scavenging systems contribute to the remarkable maintenance of ROS homeostasis in naked mole-rat brain during periods of environmental oxygen fluctuation; however, this remains to be tested. Combined with the relatively high metabolic rate of the brain[56], enhanced scavenging capacity in mitochondria support its role as the primary contributor to ROS generation in the cell. However, no study has explored the regulation of ROS generation in naked mole-rat brain.

To address this knowledge gap, we used pharmacological inhibitors of each of the key ROS generators to disrupt ROS homeostasis in naked mole-rat cortical neurons. We predicted that, as in mice and humans, pharmacological inhibition of the mitochondrial ETS would induce the most substantial fluctuations in ROS, consistent with its putative role as the primary ROS contributor in other species. We further predicted that pharmacological inhibition of XOR and NOX would similarly induce fluctuations in ROS, albeit to a lesser extent than perturbations of mitochondrial ROS homeostasis. Towards this aim, we used fluorescence microscopy to investigate fluctuations in $O_2^{\bullet-}$ and H_2O_2 production following pharmacological inhibition of the mitochondrial ETS, XOR, or NOX, in naked mole-rat cortex during a transition from normoxia to hypoxia with subsequent reoxygenation.

Materials and Methods

ANIMALS

Naked mole-rats were housed in colonies in a multi-cage system at 30°C with 21% O_2, 50% humidity, and a 12L:12D light cycle. Animals were fed vegetables, fruit, and Pronutrocereal supplement *ad libitum*. Naked mole-rats were not fasted before experiments. The Canadian Council on Animal Care and the University of Ottawa Animal Care Committee approved all experimental procedures (protocol #3444) in accordance with the Animals for Research Act.

TISSUE PREPARATION & EXPERIMENTAL DESIGN

Thirty-four subordinate adult naked mole-rats aged 1-2 years old with an average mass of 55.6 ± 19.4 g were euthanized via cervical dislocation and rapid decapitation. Brains were quickly dissected and immediately put into oxygenated (95% O_2, 5% CO_2) ice-chilled N-methyl-D-glucamine (NMDG)-based artificial cerebrospinal fluid (ACSF) where they were sliced into 300 µm thick sections by a Vibratome (Leica VT1000 S). The NMDG-based ACSF solution contained: NMDG 120 mM, NaH_2PO_4 1.25 mM, $MgCl_2$ 7 mM, $CaCl_2$ 1 mM, KCl 2.5 mM, $NaHCO_3$ 25 mM, d-glucose 20 mM, Na-pyruvate 2.4 mM, and Na-ascorbate 1.3 mM; pH 7.30 and osmolarity 315± 3 mOsM. Sections were incubated at 28°C for 30 min and then at room temperature for another 30 min, all the while in oxygenated ACSF containing: NaCl 126 mM, NaH_2PO_4 1.25 mM, $MgCl_2$ 1.5 mM, $CaCl_2$ 2 mM, KCl 2.5 mM, $NaHCO_3$ 26 mM, and d-glucose 10 mM; pH 7.30 and osmolarity 315 ± 3 mOsM. Slices were then transferred to 3 mL oxygenated ACSF baths at room temperature, individually loaded with 8 µL Cremophore EL solution (0.5% in dimethyl sulfoxide; DMSO), and then left for 5 min. 4.34 µL of 5-(and-6)-chloromethyl-2',7'-dichlorodihydrofluorescein diacetate, acetyl ester (CM-H_2DCFDA; Invitrogen, California, USA), activated in 50 µL of DMSO, was then loaded into each slice and left for 40 min.

Slices pre-loaded with CM-H_2DCFDA were placed in a chamber perfused with a 0.68 µL/mL dihydroethidium (DHE; Invitrogen, California, USA)-ACSF solution at a flow rate of ~5 mL/min. Each experiment followed a 60 min protocol; a 10 min equilibration period followed by 10 min of normoxic perfusion (DHE-ACSF), a 20 min treatment period (drug-DHE-ACSF), and finally a 20 min normoxic reperfusion period (DHE-ACSF). Control trials remained in normoxic perfusion for the entire 60 min. Hypoxic perfusion was attained by aerating ACSF with a 95% N_2, 5% CO_2 gas from a second reservoir. Drug treatments included 10 µM diphenyleneiodonium (DPI), 20 µM oxypurinol, or 0.5 µM rotenone, each dissolved in DMSO and then added to ACSF; to inhibit NOX[57], XOR[34], and complex I of the mitochondrial ETS[21], respectively.

FLUORESCENCE MICROSCOPY

Fluorescence intensity was measured using 1-min time-course images with Image-J (NIH, Bethesda, USA) to determine changes in production of whole cell H_2O_2, $O_2^{\bullet-}$, as well as mitochondrial $O_2^{\bullet-}$ in naked mole-rat cortices throughout each 60 min protocol. Images were taken with a Zeiss Axio Examiner Z1 microscope. An LED light with a 470 nm wavelength along with a 38HE filter of 500 nm-

550 nm wavelengths was used when imaging DCF dye (Zeiss, Axio Examiner Z1). When imaging MitoSOX red dye, an LED light with a 365 nm wavelength was used in conjunction with a 90HE filter containing emission wavelengths ranging 410-440 nm, 579-604 nm, and 659-759 nm (Zeiss, Axio Examiner Z1).

DATA COLLECTION & STATISTICAL ANALYSIS

Regions of interest were assigned to cortical neurons and their fluorescence was quantified. Data from each experiment were slope-corrected and normalised to baseline measurements from each experiment's initial 10 min. Fluorescence differences between drug treatments and initial normoxic exposure were analysed via two-way ANOVAs with Holm-Šídák multiple comparisons tests. Values were reported as mean ± SEM. All statistical analyses were done using GraphPad Prism 10 (GraphPad Prism, La Jolla, CA, USA), with a significance level of $p < 0.05$.

Results

Rotenone increases H_2O_2 and mitochondrial during hypoxia in naked mole-rat cortex. First, we tested the impact of complex I inhibition by rotenone on H_2O_2 and $O_2^{\bullet-}$ homeostasis during normoxia and hypoxia. Rotenone treatment did not affect H_2O_2 during normoxia, whereas hypoxic rotenone treatment led to a ~ 15% increase in H_2O_2 levels from baseline ($F_{(24,216)} = 5.183$, $p < 0.0001$), which remained stable following reoxygenation (**Fig. 1A & 1C**, n = 13 and 10 slices from 8 and 6 naked mole-rats for normoxic and normoxia-hypoxia-normoxia conditions, respectively). Similarly, mitochondrial $O_2^{\bullet-}$ was unaffected by rotenone application during normoxia, while hypoxic rotenone application elicited a 20% increase in mitochondrial $O_2^{\bullet-}$ signal above baseline ($F_{(24,192)} = 10.77$, $p < 0.0001$). However, this change was reversed following reoxygenation (**Fig. 1B & 1D**, n = 9 slices from 5 naked mole-rats for both normoxic and normoxia-hypoxia-normoxia conditions).

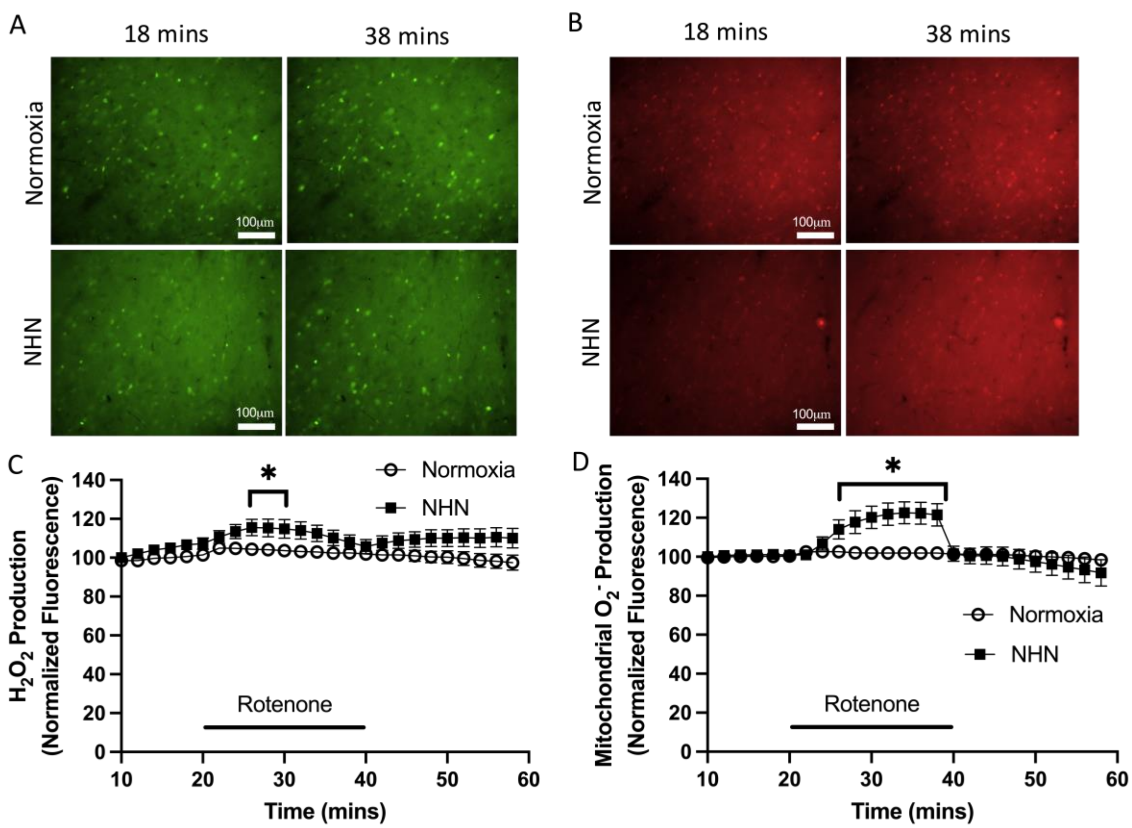

Figure 1. Rotenone induces fluctuations in hydrogen peroxide (H_2O_2) and mitochondrial superoxide ($O_2^{\bullet-}$) homeostasis in naked mole-rat (NMR) cortex during hypoxia but not normoxia. A) Fluorescent time-lapse images of cortical slices loaded with the H_2O_2 sensitive fluorophore CM-H_2-DCFDA, and **B)** the $O_2^{\bullet-}$ sensitive mitochondrial fluorophore MitoSOX Red, prior to and during rotenone application, while exposed to normoxia or a normoxia-hypoxia-normoxia (NHN) protocol. **C)** Summary of H_2O_2 fluctuations with rotenone application in normoxia and hypoxia (n = 13 and 10 slices from 8 and 6 NMRs for normoxic and NHN conditions, respectively). **D)** Summary of mitochondrial $O_2^{\bullet-}$ fluctuations with rotenone application in normoxia and hypoxia (n = 9 slices from 5 NMRs for both normoxic and NHN conditions). Individual trials were slope-corrected and normalised based on the initial 10-min normoxic period. Black bars indicate rotenone treatment during normoxia (open circles), and hypoxia (black squares). Asterisks indicate

significant differences from initial normoxic values ($p < 0.05$; Two-way ANOVA with Holm-Šídák multiple comparisons test). Data are presented as mean ± SEM.

Oxypurinol elevates $O_2^{\bullet-}$, but not H_2O_2, during both normoxia and hypoxia. Next, we evaluated the role of XOR in ROS homeostasis through inhibition with oxypurinol during normoxia and hypoxia. Treatment with oxypurinol had no significant effect on H_2O_2 levels during normoxia or hypoxia (**Fig. 2A & 2C**, n = 11 and 11 slices from 7 and 9 naked mole-rats for normoxic and normoxia-hypoxia-normoxia conditions, respectively). In contrast, oxypurinol elevated $O_2^{\bullet-}$ by ~ 100% and ~ 70% above baseline during normoxic and hypoxic exposure, respectively ($F_{(59,413)} = 58.74$, $p < 0.0001$; and $F_{(59,354)} = 29.54$, $p < 0.0001$, respectively). $O_2^{\bullet-}$ levels then dropped to ~ 50% and ~ 30% above baseline following reperfusion after normoxic and hypoxic drug applications, respectively (**Fig. 2B & 2D**, n = 6 and 7 slices from 3 and 5 naked mole-rats for normoxic and normoxia-hypoxia-normoxia conditions, respectively).

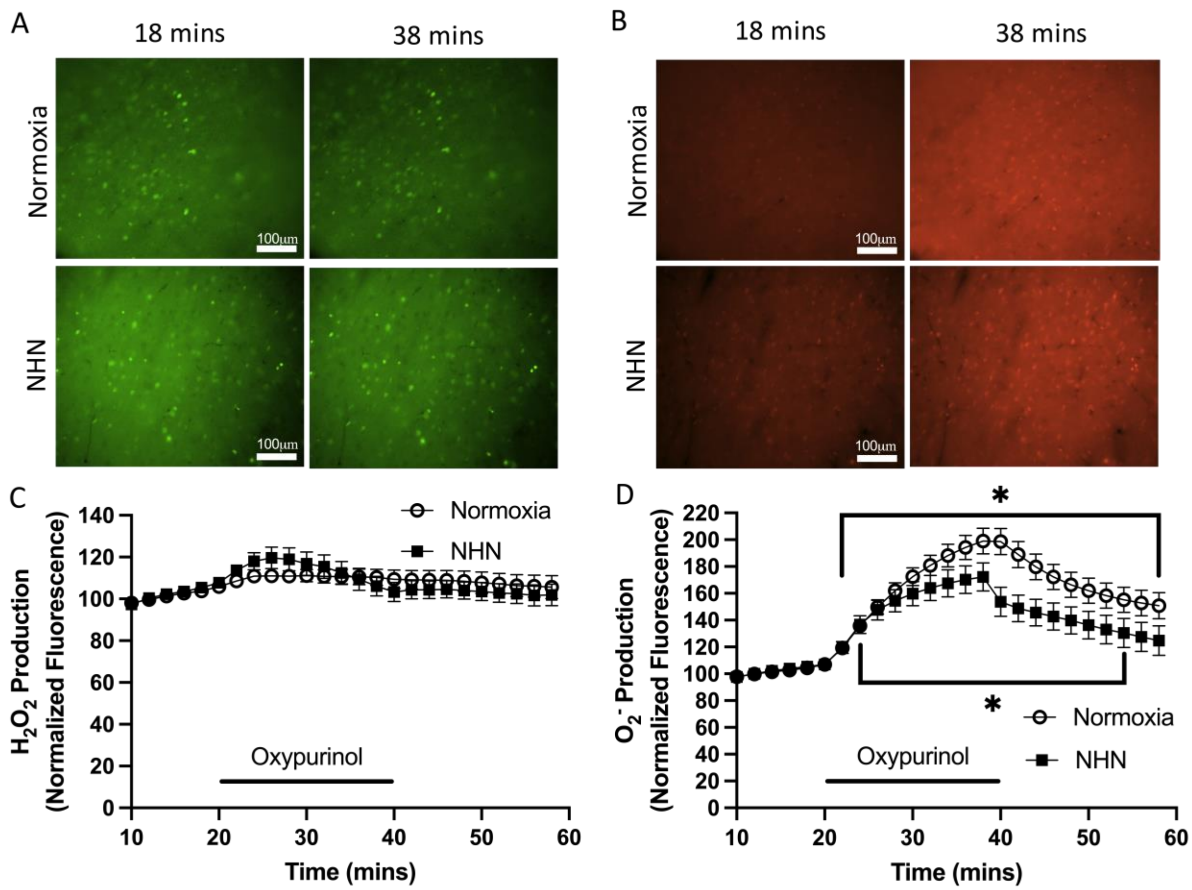

Figure 2. Oxypurinol induces fluctuations in hydrogen peroxide (H_2O_2) and superoxide ($O_2^{\bullet-}$) homeostasis in naked mole-rat (NMR) cortex during hypoxia and normoxia. A) Fluorescent time-lapse images of cortical slices loaded with the H_2O_2 sensitive fluorophore CM-H_2-DCFDA, and **B)** the $O_2^{\bullet-}$ sensitive fluorophore dihydroethidium, prior to and during oxypurinol application, while exposed to normoxia or a normoxia-hypoxia-normoxia (NHN) protocol. **C)** Summary of H_2O_2 fluctuations with oxypurinol application in normoxia and hypoxia (n = 11 and 11 slices from 7 and 9 NMRs for normoxic and NHN conditions, respectively). **D)** Summary of $O_2^{\bullet-}$ fluctuations with oxypurinol application in normoxia and hypoxia (n = 6 and 7 slices from 3 and 5 NMRs for normoxic and NHN conditions, respectively). Individual trials were slope-corrected and normalised based on the initial 10-min normoxic period. Black bars indicate oxypurinol treatment during normoxia (open circles), and hypoxia (black squares). Asterisks indicate significant differences from initial normoxic values ($p < 0.05$; Two-way ANOVA with Holm-Šídák multiple comparisons test). Data are presented as mean ± SEM.

Diphenyleneiodonium application during hypoxia disrupts reactive oxygen species homeostasis. Finally, we inhibited NOX with DPI to examine the impact of this treatment on H_2O_2 and $O_2^{\bullet-}$ homeostasis in naked mole-rat cortex during normoxic and hypoxic exposure. Diphenyleneiodonium treatment had no effect on normoxic H_2O_2 homeostasis, however DPI treatment during hypoxia resulted in a ~ 35% decrease in fluorescent signal compared to baseline ($F_{(24,144)} = 20.21$, $p < 0.0001$), which remained stable following reoxygenation (**Fig. 3A & 3C**, n = 5 and 7 slices from 4 and 5 naked mole-rats for normoxic and normoxia-hypoxia-normoxia conditions, respectively). Normoxic DPI application also had no effect on $O_2^{\bullet-}$ homeostasis. Conversely, DPI application during hypoxia elevated $O_2^{\bullet-}$ levels by ~ 30% from baseline ($F_{(24,144)} = 6.995$, $p < 0.0001$), although $O_2^{\bullet-}$ levels returned to baseline following reoxygenation (**Fig. 3B & 3D**, n = 5 and 7 slices from 4 and 4 naked mole-rats for normoxic and normoxia-hypoxia-normoxia conditions, respectively).

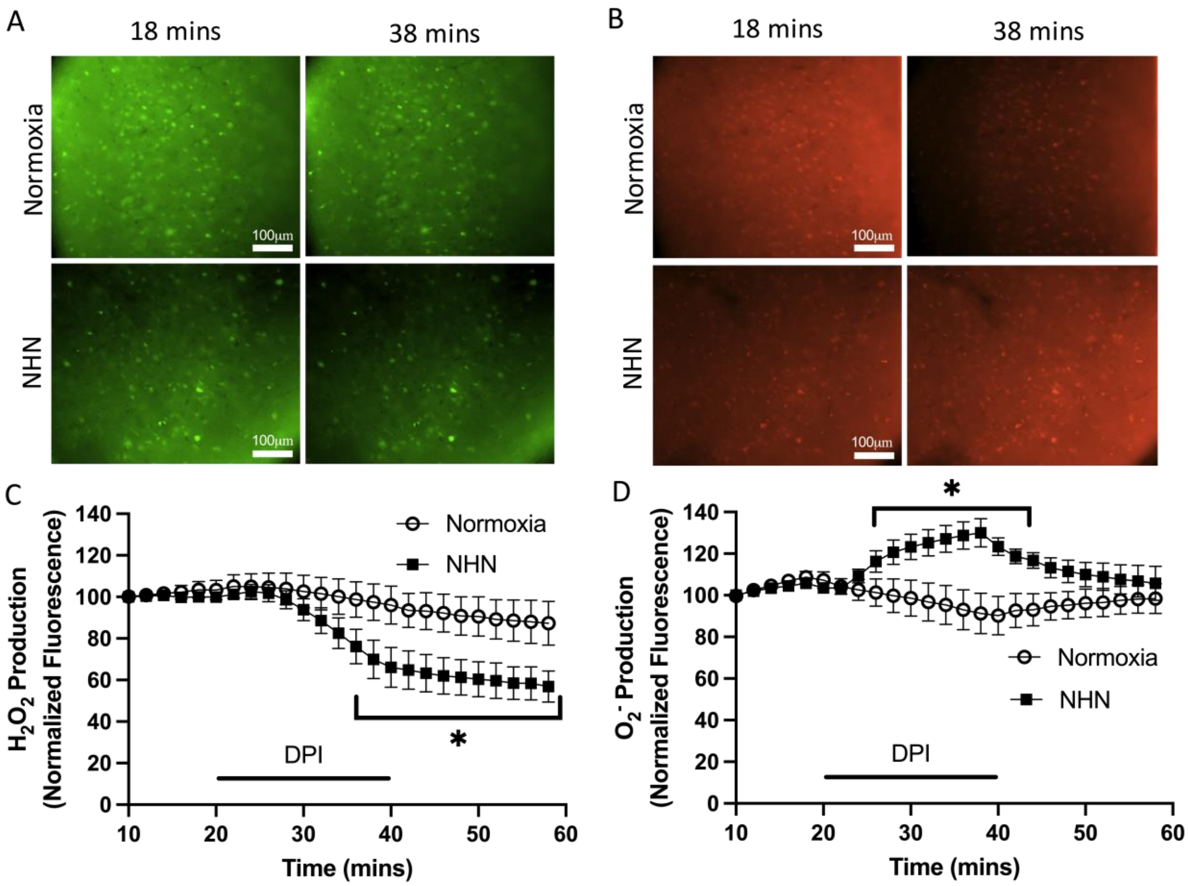

Figure 3. Diphenyleneiodonium (DPI) induces fluctuations in hydrogen peroxide (H_2O_2) and superoxide ($O_2^{\bullet-}$) homeostasis in naked mole-rat (NMR) cortex during hypoxia but not normoxia. A) Fluorescent time-lapse images of cortical slices loaded with the H_2O_2 sensitive fluorophore CM-H_2-DCFDA, and **B)** the $O_2^{\bullet-}$ sensitive fluorophore dihydroethidium, prior to and during DPI application, while exposed to normoxia or a normoxia-hypoxia-normoxia (NHN) protocol. **C)** Summary of H_2O_2 fluctuations with DPI application in normoxia and hypoxia (n = 5 and 7 slices from 4 and 5 NMRs for normoxic and NHN conditions, respectively). **D)** Summary of $O_2^{\bullet-}$ fluctuations with DPI application in normoxia and hypoxia (n = 5 and 7 slices from 4 and 4 NMRs for normoxic and NHN conditions, respectively). Individual trials were slope-corrected and normalised based on the initial 10-min normoxic period. Black bars indicate DPI treatment during normoxia (open circles), and hypoxia (black squares). Asterisks indicate significant differences from initial normoxic values ($p < 0.05$; Two-way ANOVA with Holm-Šídák multiple comparisons test). Data are presented as mean ± SEM.

Discussion

We measured fluctuations in ROS levels following pharmacological inhibition of three key ROS generators (XOR, NOX, and mitochondrial complex I) during normoxia and hypoxia to determine their relative contributions to ROS homeostasis in naked mole-rat cortex. We report two key but unexpected findings. First, inhibition of XOR during normoxia leads to a substantial increase in $O_2^{\bullet-}$, whereas inhibition of mitochondrial complex I or NOX during normoxia did not induce any fluctuations in ROS. Second, inhibition of each ROS generator during hypoxia elevates $O_2^{\bullet-}$ levels, with XOR inhibition eliciting a greater increase in $O_2^{\bullet-}$

than inhibition of mitochondrial complex I or NOX; and NOX inhibition leading to decreased H_2O_2 levels in hypoxia. Thus contrary to our initial hypothesis, our findings suggest that XOR plays a more substantial role in ROS generation in naked mole-rat brain than does mitochondria complex I and NOX.

Normoxic inhibition of xanthine oxidoreductase, but not mitochondrial complex I, induces large fluctuations in $O_2^{\bullet-}$. Of the three ROS generators manipulated in our study, only pharmacological inhibition of XOR induces a substantial increase in $O_2^{\bullet-}$ in the normoxic naked mole-rat cortex, whereas H_2O_2 remains relatively unchanged. Conversely, pharmacological inhibition of mitochondrial complex I or NOX during normoxia does not induce substantial fluctuations in ROS production in cortex (**Fig. 4** and see below). These observations are unlike previous studies in hypoxia-intolerant rodent brains which report that XOR usually produces ROS as a by-product of purine catabolism and is not a primary contributor to ROS generation during normoxia in mouse (*Mus musculus*) brain[31,58]. Indeed, pharmacological inhibition of XOR with oxypurinol administration is not neuroprotective in neo-natal rat pups following ischemic insult[59].

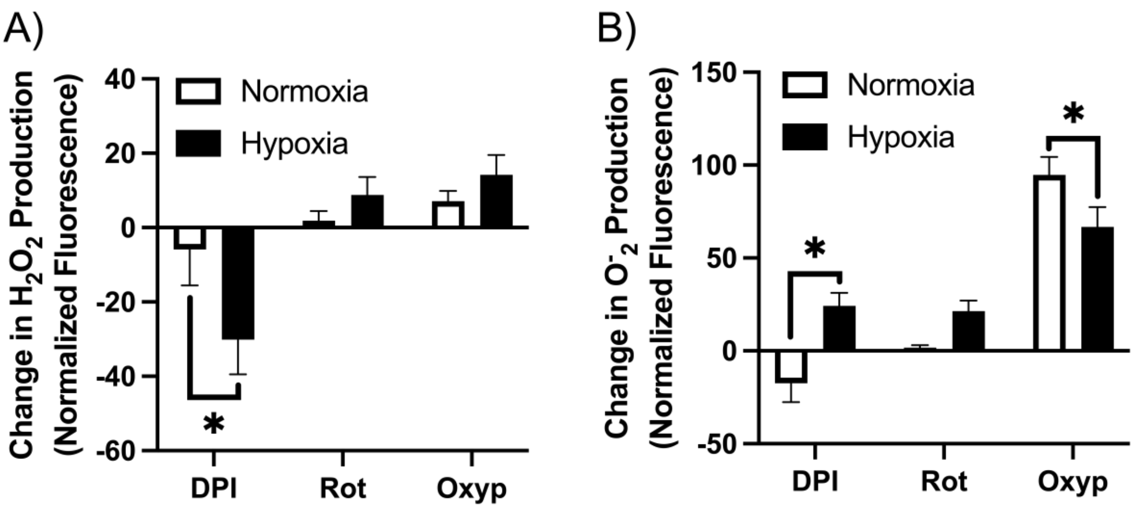

Figure 4. Fluctuations in A) hydrogen peroxide (H_2O_2) and B) superoxide ($O_2^{\bullet-}$) production from initial normoxic values following normoxic and hypoxic inhibition of generators in cortex of naked mole-rats. Rot=Rotenone, Oxyp=Oxypurinol, DPI=Diphenyleneiodonium. Letters indicate significant difference between oxygen levels and drug treatments ($p < 0.05$; Two-way ANOVA with Holm-Šídák multiple comparisons test). Data presented as differences between mean values ± SEM within each condition.

Importantly, in addition to producing hypoxanthine, XOR also produces uric acid, which helps maintain antioxidant capacity[60], and which has been suggested to have neuroprotective antioxidant properties in cultured rat hippocampal neurons[61,62]. Indeed, although uric acid is primarily a waste product, it also scavenges $O_2^{\bullet-}$, hydroxyl radicals, and singlet oxygen[63,64]. Uric acid may also prevent the degradation of superoxide dismutase, an important ROS scavenging enzyme responsible for dismutating $O_2^{\bullet-}$ into less harmful H_2O_2[65]. As such, inhibiting XOR may deprive cells of an important purine and compromise ROS scavenging capacity, which may explain the large increase in $O_2^{\bullet-}$ we observe following application of oxypurinol. Further investigations into the roles of XOR and uric acid in brain ROS homeostasis are warranted.

The absence of fluctuating ROS levels in naked mole-rat cortex following complex I inhibition also differs from previous reports in hypoxia-intolerant rodent brain. For example, application of rotenone during normoxia leads to elevated ROS production in mouse brain[66-69]. One potential explanation for this discrepancy is that naked mole-rat brain mitochondria have an enhanced ROS scavenging capacity relative to hypoxia-intolerant species[45]. It is possible that naked mole-rat brain mitochondria avoid excess ROS production, even during rotenone application, through similarly improved scavenging capacity. Similarly, our results we present here and previous work suggest that NOX is not a major ROS generator in naked mole-rat brain[70], unless NOX is recruited as part of an immune response or for protein folding and steroid biosynthesis[35,37,38].

Hypoxic inhibition of xanthine oxidoreductase induces the largest fluctuation in reactive oxygen species. While inhibiting each source of ROS generation during hypoxia led to significant fluctuations in both H_2O_2 and $O_2^{\bullet-}$, hypoxic inhibition of XOR induced a comparatively greater increase in $O_2^{\bullet-}$, while H_2O_2 was maintained (**Fig. 4**). As with our normoxic results, this observation is in stark contrast to previous reports on brains of hypoxia-intolerant rodents. For example, although XOR-generated ROS does increase in rat hippocampal and cortical neuronal cultures when exposed to OGD, this contribution to total cellular ROS generation is less than the contributions of mitochondria and NOX[34]. Similarly in mouse brain, XOR partially contributes to $O_2^{\bullet-}$ generation during hypoxic or ischemic conditions, but XOR expression is low compared to other tissues[58]. Moreover, oxypurinol administration is not neuroprotective following ischemic insult in neo-natal rat pups, suggesting a negligible contribution of XOR to deleterious ROS production in hypoxic brain[59]. Similarly, XOR-generated ROS does not appear to be involved in the activation of apoptosis following *in-vivo* hypoxia-ischemia exposure in rabbit (*Oryctolagus cuniculus*) brain[71]. Unfortunately, XOR and its purine catabolites have not been investigated in the brains of naked mole-rats. However, naked mole-rats have been reported to metabolize fructose for glycolysis in severely hypoxic or anoxic conditions[72]. Xanthine can be produced during fructose metabolism, which may fuel XOR activity and further provide the hypoxic naked mole-rat brain with uric acid to bolster antioxidant capacity[73]. Future studies investigating this possible link are warranted.

Hypoxic inhibition of mitochondrial complex I yielded significant fluctuations in both H_2O_2 and $O_2^{\bullet-}$, albeit to a lesser degree than both XOR and NOX (**Fig. 4**). Many hypoxia-tolerant animals have adaptions that mediate the potentially lethal accumulation of oxidative damage by decreasing or sustaining (i.e., avoiding increases in) mitochondrial ROS generation during low-oxygen conditions[44]. For example, permeabilized ventricles fibres of the hypoxia-tolerant epaulette shark (*Hemiscyllium ocellatum*) produce 50%-25% less H_2O_2 than those of the hypoxia-intolerant shovelnose ray (*Aptychotrema rostrata*) during normoxic conditions and after acute hypoxic exposure (2 h at 2 and 3 kPa O_2, respectively)[42]. Similar adaptations have been found in the thoracic muscles of hypoxia-adapted fruit flies (*Drosophila melanogaster*)[74], skeletal muscle of deer mice (*Peromyscus maniculatus*)[50], and in the liver of killifish (*Fundulus heteroclitus*)[47]. Naked mole-rats fit in this general pattern of constraining ROS surges during hypoxia. Compared to mice, naked mole-rats have a ~75% lower basal metabolic rate, produce less mitochondrial ROS in normoxia, further reduce brain respiratory flux through the ETS by nearly 90% during hypoxia, and naked mole-rat cortex does not exhibit fluctuations in mitochondrial $O_2^{\bullet-}$ during hypoxia[40,75-77]. Thus, our results suggest that limiting perturbations in cortical mitochondrial ROS production plays a role in maintaining ROS homeostasis.

Finally, and unlike in other hypoxic experiments, pharmacological inhibition of NOX with DPI unexpectedly induces a substantial decrease in H_2O_2, and a contrasting increase in $O_2^{\bullet-}$ during hypoxia (**Fig. 4**). While NOX is responsible for some H_2O_2 production, the primary form of ROS produced by NOX is $O_2^{\bullet-}$[57,78]. A reperfusion-mediated burst in ROS following hypoxic exposure is also attributed to NOX[34,79], however a succinate-driven mitochondrial mechanism has also been proposed as the primary source of ROS surges during reperfusion[26]. Thus, our understanding of the source of this reperfusion-mediated burst in ROS remains inconclusive. Treatment with DPI during ischemia diminishes $O_2^{\bullet-}$ upon reperfusion in rat neuronal cultures, and ischemic lesion size in rat brains[34,80,81]. Conversely, we observe only a contrasting increase in $O_2^{\bullet-}$ during hypoxic application of DPI and a non-significant decrease during normoxic application. Regardless of what mechanism may drive this reperfusion-mediated ROS burst, neither our previous nor current findings support the presence of any ROS burst upon reperfusion in naked mole-rat cortex[40]. In line with our predictions, and when compared to XOR and mitochondrial complex I, NOX at least partly contributes to hypoxic ROS generation. However, our results overall do not align with previous literature and suggest a greater role of XOR in ROS generation in naked mole-rat brain.

Study limitations and future directions. Our study relies on pharmacological tools, which can elicit unexpected and off-target effects. For example, DPI is a broad flavoprotein inhibitor that potently targets all NOX isoforms by covalently bonding to the flavin adenine dinucleotide domain, effectively mediating the production of $O_2^{\bullet-}$ via electron transfer to O_2[57,78,82]. The $O_2^{\bullet-}$ that would otherwise be produced by NOX is then quickly dismutated into H_2O_2. As such, inhibition of NOX with DPI may attenuate H_2O_2 production and concomitant hypoxic exposure may exacerbate this drop in H_2O_2. Our observations are consistent with this proposed mechanism. However, DPI can also interact with other flavoprotein-containing enzymes such as nitric oxide synthase, XOR, and mitochondrial complex I[83-85]. Furthermore, DPI may bind to the same site of mitochondrial complex I as rotenone[21,83]. If DPI is inhibiting mitochondrial complex I in addition to NOX in naked mole-rat cortex, this may explain the similar trends observed between hypoxic application of DPI and rotenone on $O_2^{\bullet -}$ homeostasis. However, some fluctuations we observed during DPI application are unlike those resulting from rotenone or oxypurinol treatments, suggesting that this is unlikely. Alternatively, NOX inhibition with DPI may shunt NADPH to GSH and Trx-dependent ROS scavenging pathways, effectively attenuating ROS production while simultaneously promoting ROS scavenging.

Conclusions. Naked mole-rats are remarkably hypoxia-tolerant mammals. Given the central role of excessive ROS generation in hypoxic brain cell death, the ability of naked mole-rat brain to maintain ROS homeostasis is likely a fundamental pillar in their ability to withstand intermittent and severe hypoxia. We set out to determine the relative contributions of the primary cellular ROS generators to normoxic and hypoxic ROS production in naked mole-rat brain. Contrary to our hypothesis, and unlike in the brains of most hypoxia-intolerant mammals, mitochondrial ROS homeostasis was the least perturbed in both normoxic and hypoxic conditions. Instead, pharmacological inhibition of XOR yielded the most substantial fluctuations in ROS during both normoxic and hypoxic treatments in naked mole-rat cortex. These findings highlight the interconnectivity of ROS-mediated adaptations to hypoxia, and how multiple systems may contribute to improved ROS homeostasis in species adapted to environments with varying oxygen availability.

Funding

This work was supported by an NSERC Discovery grant (#04229), an Ontario Early Career Research Award, and an NIHRO3 grant (#AG052390) to MEP, and an Ontario Graduate Scholarship to LE.

Competing Interests

We have no competing interests.

Acknowledgements

We would like to thank the uOttawa veterinary technicians for their assistance in animal handling and husbandry.

Author Contributions

LE and MEP conceived and designed the study. LE, IW, JB, and AKH conducted experiments. LE and IW analyzed data. LE, JB, and MEP wrote the manuscript and LE, IW, and MEP edited and approved of the manuscript in its final form.

References

1. Wang Y, Zang QS, Liu Z, et al. Regulation of VEGF-induced endothelial cell migration by mitochondrial reactive oxygen species. *Am J Physiol Cell Physiol*. Sep 2011;301(3):C695-704. doi:10.1152/ajpcell.00322.2010
2. West AP, Shadel GS, Ghosh S. Mitochondria in innate immune responses. *Nat Rev Immunol*. Jun 2011;11(6):389-402. doi:10.1038/nri2975
3. Finkel T. Signal transduction by mitochondrial oxidants. *J Biol Chem*. Feb 10 2012;287(7):4434-40. doi:10.1074/jbc.R111.271999
4. Kiselyov K, Muallem S. ROS and intracellular ion channels. *Cell Calcium*. Aug 2016;60(2):108-14. doi:10.1016/j.ceca.2016.03.004
5. Scherz-Shouval R, Shvets E, Fass E, Shorer H, Gil L, Elazar Z. Reactive oxygen species are essential for autophagy and specifically regulate the activity of Atg4. *EMBO J*. Apr 4 2007;26(7):1749-60. doi:10.1038/sj.emboj.7601623
6. Starkov AA, Andreyev AY, Zhang SF, et al. Scavenging of H2O2 by mouse brain mitochondria. *J Bioenerg Biomembr*. Dec 2014;46(6):471-7. doi:10.1007/s10863-014-9581-9
7. Munro D, Banh S, Sotiri E, Tamanna N, Treberg JR. The thioredoxin and glutathione-dependent H2O2 consumption pathways in muscle mitochondria: Involvement in H2O2 metabolism and consequence to H2O2 efflux assays. *Free Radic Biol Med*. Jul 2016;96:334-46. doi:10.1016/j.freeradbiomed.2016.04.014
8. Drechsel DA, Patel M. Respiration-dependent H2O2 removal in brain mitochondria via the thioredoxin/peroxiredoxin system. *J Biol Chem*. Sep 3 2010;285(36):27850-8. doi:10.1074/jbc.M110.101196
9. Guzy RD, Hoyos B, Robin E, et al. Mitochondrial complex III is required for hypoxia-induced ROS production and cellular oxygen sensing. *Cell Metab*. Jun 2005;1(6):401-8. doi:10.1016/j.cmet.2005.05.001
10. Panov A, Dikalov S, Shalbuyeva N, Hemendinger R, Greenamyre JT, Rosenfeld J. Species- and tissue-specific relationships between mitochondrial permeability transition and generation of ROS in brain and liver mitochondria of rats and mice. *Am J Physiol Cell Physiol*. Feb 2007;292(2):C708-18. doi:10.1152/ajpcell.00202.2006
11. Wang F, Wang X, Liu Y, Zhang Z. Effects of Exercise-Induced ROS on the Pathophysiological Functions of Skeletal Muscle. *Oxid Med Cell Longev*. 2021;2021:3846122. doi:10.1155/2021/3846122
12. Marchi S, Giorgi C, Suski JM, et al. Mitochondria-ros crosstalk in the control of cell death and aging. *J Signal Transduct*. 2012;2012:329635. doi:10.1155/2012/329635
13. Apel K, Hirt H. Reactive oxygen species: metabolism, oxidative stress, and signal transduction. *Annu Rev Plant Biol*. 2004;55:373-99. doi:10.1146/annurev.arplant.55.031903.141701
14. Levraut J, Iwase H, Shao ZH, Vanden Hoek TL, Schumacker PT. Cell death during ischemia: relationship to mitochondrial depolarization and ROS generation. *Am J Physiol Heart Circ Physiol*. Feb 2003;284(2):H549-58. doi:10.1152/ajpheart.00708.2002
15. Adam-Vizi V. Production of reactive oxygen species in brain mitochondria: contribution by electron transport chain and non-electron transport chain sources. *Antioxid Redox Signal*. Sep-Oct 2005;7(9-10):1140-9. doi:10.1089/ars.2005.7.1140
16. Aon MA, Stanley BA, Sivakumaran V, et al. Glutathione/thioredoxin systems modulate mitochondrial H2O2 emission: an experimental-computational study. *J Gen Physiol*. Jun 2012;139(6):479-91. doi:10.1085/jgp.201210772
17. Chance B, Sies H, Boveris A. Hydroperoxide metabolism in mammalian organs. *Physiol Rev*. Jul 1979;59(3):527-605. doi:10.1152/physrev.1979.59.3.527
18. Zorov DB, Juhaszova M, Sollott SJ. Mitochondrial reactive oxygen species (ROS) and ROS-induced ROS release. *Physiol Rev*. Jul 2014;94(3):909-50. doi:10.1152/physrev.00026.2013
19. Turrens JF, Freeman BA, Levitt JG, Crapo JD. The effect of hyperoxia on superoxide production by lung submitochondrial particles. *Arch Biochem Biophys*. Sep 1982;217(2):401-10. doi:10.1016/0003-9861(82)90518-5
20. Wilson DF, Rumsey WL, Green TJ, Vanderkooi JM. The oxygen dependence of mitochondrial oxidative phosphorylation measured by a new optical method for measuring oxygen concentration. *J Biol Chem*. Feb 25 1988;263(6):2712-8.
21. Orr AL, Ashok D, Sarantos MR, Shi T, Hughes RE, Brand MD. Inhibitors of ROS production by the ubiquinone-binding site of mitochondrial complex I identified by chemical screening. *Free Radic Biol Med*. Dec 2013;65:1047-1059. doi:10.1016/j.freeradbiomed.2013.08.170
22. Scialo F, Fernandez-Ayala DJ, Sanz A. Role of Mitochondrial Reverse Electron Transport in ROS Signaling: Potential Roles in Health and Disease. *Front Physiol*. 2017;8:428. doi:10.3389/fphys.2017.00428
23. Chandel NS, Maltepe E, Goldwasser E, Mathieu CE, Simon MC, Schumacker PT.

Mitochondrial reactive oxygen species trigger hypoxia-induced transcription. *Proc Natl Acad Sci U S A*. Sep 29 1998;95(20):11715-20. doi:10.1073/pnas.95.20.11715
24. Paddenberg R, Ishaq B, Goldenberg A, et al. Essential role of complex II of the respiratory chain in hypoxia-induced ROS generation in the pulmonary vasculature. *Am J Physiol Lung Cell Mol Physiol*. May 2003;284(5):L710-9. doi:10.1152/ajplung.00149.2002
25. Quinlan CL, Orr AL, Perevoshchikova IV, Treberg JR, Ackrell BA, Brand MD. Mitochondrial complex II can generate reactive oxygen species at high rates in both the forward and reverse reactions. *J Biol Chem*. Aug 3 2012;287(32):27255-64. doi:10.1074/jbc.M112.374629
26. Chouchani ET, Pell VR, James AM, et al. A Unifying Mechanism for Mitochondrial Superoxide Production during Ischemia-Reperfusion Injury. *Cell Metab*. Feb 9 2016;23(2):254-63. doi:10.1016/j.cmet.2015.12.009
27. Bayir H. Reactive oxygen species. *Crit Care Med*. Dec 2005;33(12 Suppl):S498-501. doi:10.1097/01.ccm.0000186787.64500.12
28. Kishida KT, Klann E. Sources and targets of reactive oxygen species in synaptic plasticity and memory. *Antioxid Redox Signal*. Feb 2007;9(2):233-44. doi:10.1089/ars.2007.9.ft-8
29. Berry CE, Hare JM. Xanthine oxidoreductase and cardiovascular disease: molecular mechanisms and pathophysiological implications. *J Physiol*. Mar 16 2004;555(Pt 3):589-606. doi:10.1113/jphysiol.2003.055913
30. Collin F. Chemical Basis of Reactive Oxygen Species Reactivity and Involvement in Neurodegenerative Diseases. *Int J Mol Sci*. May 15 2019;20(10)doi:10.3390/ijms20102407
31. Hille R, Hall J, Basu P. The mononuclear molybdenum enzymes. *Chem Rev*. Apr 9 2014;114(7):3963-4038. doi:10.1021/cr400443z
32. Godber BL, Doel JJ, Sapkota GP, et al. Reduction of nitrite to nitric oxide catalyzed by xanthine oxidoreductase. *J Biol Chem*. Mar 17 2000;275(11):7757-63. doi:10.1074/jbc.275.11.7757
33. Nanduri J, Vaddi DR, Khan SA, et al. HIF-1alpha activation by intermittent hypoxia requires NADPH oxidase stimulation by xanthine oxidase. *PLoS One*. 2015;10(3):e0119762. doi:10.1371/journal.pone.0119762
34. Abramov AY, Scorziello A, Duchen MR. Three distinct mechanisms generate oxygen free radicals in neurons and contribute to cell death during anoxia and reoxygenation. *J Neurosci*. Jan 31 2007;27(5):1129-38. doi:10.1523/JNEUROSCI.4468-06.2007
35. Babior BM. The respiratory burst oxidase. *Adv Enzymol Relat Areas Mol Biol*. 1992;65:49-95. doi:10.1002/9780470123119.ch2
36. Vignais PV. The superoxide-generating NADPH oxidase: structural aspects and activation mechanism. *Cell Mol Life Sci*. Sep 2002;59(9):1428-59. doi:10.1007/s00018-002-8520-9
37. Mennerich D, Kellokumpu S, Kietzmann T. Hypoxia and Reactive Oxygen Species as Modulators of Endoplasmic Reticulum and Golgi Homeostasis. *Antioxid Redox Signal*. Jan 1 2019;30(1):113-137. doi:10.1089/ars.2018.7523
38. Sies H, Belousov VV, Chandel NS, et al. Defining roles of specific reactive oxygen species (ROS) in cell biology and physiology. *Nat Rev Mol Cell Biol*. Feb 21 2022;doi:10.1038/s41580-022-00456-z
39. Welker AF, Campos EG, Cardoso LA, Hermes-Lima M. Role of catalase on the hypoxia/reoxygenation stress in the hypoxia-tolerant Nile tilapia. *Am J Physiol Regul Integr Comp Physiol*. May 2012;302(9):R1111-8. doi:10.1152/ajpregu.00243.2011
40. Eaton L, Wang T, Roy M, Pamenter ME. Naked Mole-Rat Cortex Maintains Reactive Oxygen Species Homeostasis During In Vitro Hypoxia or Ischemia and Reperfusion. *Curr Neuropharmacol*. 2023;21(6):1450-1461. doi:10.2174/1570159X20666220327220929
41. Pamenter ME, Richards MD, Buck LT. Anoxia-induced changes in reactive oxygen species and cyclic nucleotides in the painted turtle. *J Comp Physiol B*. May 2007;177(4):473-81. doi:10.1007/s00360-007-0145-8
42. Hickey AJ, Renshaw GM, Speers-Roesch B, et al. A radical approach to beating hypoxia: depressed free radical release from heart fibres of the hypoxia-tolerant epaulette shark (Hemiscyllum ocellatum). *J Comp Physiol B*. Jan 2012;182(1):91-100. doi:10.1007/s00360-011-0599-6
43. Buffenstein R. Negligible senescence in the longest living rodent, the naked mole-rat: insights from a successfully aging species. *J Comp Physiol B*. May 2008;178(4):439-45. doi:10.1007/s00360-007-0237-5
44. Eaton L, Pamenter ME. What to do with low O2: Redox adaptations in vertebrates native to hypoxic environments. *Comp Biochem Physiol A Mol Integr Physiol*. Sep 2022;271:111259. doi:10.1016/j.cbpa.2022.111259
45. Munro D, Baldy C, Pamenter ME, Treberg JR. The exceptional longevity of the naked mole-rat may be explained by mitochondrial antioxidant defenses. *Aging Cell*. Jun 2019;18(3):e12916. doi:10.1111/acel.12916

46. Schulke S, Dreidax D, Malik A, et al. Living with stress: regulation of antioxidant defense genes in the subterranean, hypoxia-tolerant mole rat, Spalax. *Gene*. Jun 1 2012;500(2):199-206. doi:10.1016/j.gene.2012.03.019
47. Du SN, Mahalingam S, Borowiec BG, Scott GR. Mitochondrial physiology and reactive oxygen species production are altered by hypoxia acclimation in killifish (Fundulus heteroclitus). *J Exp Biol*. Apr 15 2016;219(Pt 8):1130-8. doi:10.1242/jeb.132860
48. Reiterer M, Milton SL. Induction of foxo3a protects turtle neurons against oxidative stress. *Comp Biochem Physiol A Mol Integr Physiol*. May 2020;243:110671. doi:10.1016/j.cbpa.2020.110671
49. Lushchak VI, Lushchak LP, Mota AA, Hermes-Lima M. Oxidative stress and antioxidant defenses in goldfish Carassius auratus during anoxia and reoxygenation. *Am J Physiol Regul Integr Comp Physiol*. Jan 2001;280(1):R100-7. doi:10.1152/ajpregu.2001.280.1.R100
50. Mahalingam S, McClelland GB, Scott GR. Evolved changes in the intracellular distribution and physiology of muscle mitochondria in high-altitude native deer mice. *J Physiol*. Jul 15 2017;595(14):4785-4801. doi:10.1113/JP274130
51. Pamenter ME. Adaptations to a hypoxic lifestyle in naked mole-rats. *J Exp Biol*. Feb 15 2022;225(4)doi:10.1242/jeb.196725
52. Buffenstein R, Amoroso V, Andziak B, et al. The naked truth: a comprehensive clarification and classification of current 'myths' in naked mole-rat biology. *Biol Rev Camb Philos Soc*. Feb 2022;97(1):115-140. doi:10.1111/brv.12791
53. Cheng H, Pamenter ME. Naked mole-rat brain mitochondria tolerate in vitro ischaemia. *J Physiol*. Oct 2021;599(20):4671-4685. doi:10.1113/JP281942
54. Wang TH, Eaton L, Pamenter ME. Nitric oxide homeostasis is maintained during acute in vitro hypoxia and following reoxygenation in naked mole-rat but not mouse cortical neurons. *Comp Biochem Physiol A Mol Integr Physiol*. Dec 2020;250:110792. doi:10.1016/j.cbpa.2020.110792
55. Hadj-Moussa H, Eaton L, Cheng H, Pamenter ME, Storey KB. Naked mole-rats resist the accumulation of hypoxia-induced oxidative damage. *Comp Biochem Physiol A Mol Integr Physiol*. Nov 2022;273:111282. doi:10.1016/j.cbpa.2022.111282
56. Vakharia K, Shallwani H, Beecher JS, Jowdy PK, Levy EI. 23 - Endovascular Treatment of Acute Stroke and Occlusive Cerebrovascular Disease. In: Ellenbogen RG, Sekhar LN, Kitchen ND, da Silva HB, eds. *Principles of Neurological Surgery (Fourth Edition)*. Elsevier; 2018:343-354.e4.
57. Augsburger F, Filippova A, Rasti D, et al. Pharmacological characterization of the seven human NOX isoforms and their inhibitors. *Redox Biology*. 2019/09/01/ 2019;26:101272. doi:https://doi.org/10.1016/j.redox.2019.101272
58. Suzuki G, Okamoto K, Kusano T, Matsuda Y, Fuse A, Yokota H. Evaluation of neuronal protective effects of xanthine oxidoreductase inhibitors on severe whole-brain ischemia in mouse model and analysis of xanthine oxidoreductase activity in the mouse brain. *Neurol Med Chir (Tokyo)*. 2015;55(1):77-85. doi:10.2176/nmc.oa.2013-0307
59. Feng Y, Shi W, Huang M, LeBlanc MH. Oxypurinol administration fails to prevent hypoxic-ischemic brain injury in neonatal rats. *Brain Res Bull*. Feb 15 2003;59(6):453-7. doi:10.1016/s0361-9230(02)00963-2
60. Garcia-Gil M, Camici M, Allegrini S, Pesi R, Petrotto E, Tozzi MG. Emerging Role of Purine Metabolizing Enzymes in Brain Function and Tumors. *Int J Mol Sci*. Nov 14 2018;19(11)doi:10.3390/ijms19113598
61. Mijailovic NR, Vesic K, Borovcanin MM. The Influence of Serum Uric Acid on the Brain and Cognitive Dysfunction. *Front Psychiatry*. 2022;13:828476. doi:10.3389/fpsyt.2022.828476
62. Yu ZF, Bruce-Keller AJ, Goodman Y, Mattson MP. Uric acid protects neurons against excitotoxic and metabolic insults in cell culture, and against focal ischemic brain injury in vivo. *J Neurosci Res*. Sep 1 1998;53(5):613-25. doi:10.1002/(SICI)1097-4547(19980901)53:5<613::AID-JNR11>3.0.CO;2-1
63. Ames BN, Cathcart R, Schwiers E, Hochstein P. Uric acid provides an antioxidant defense in humans against oxidant- and radical-caused aging and cancer: a hypothesis. *Proc Natl Acad Sci U S A*. Nov 1981;78(11):6858-62. doi:10.1073/pnas.78.11.6858
64. Kutzing MK, Firestein BL. Altered uric acid levels and disease states. *J Pharmacol Exp Ther*. Jan 2008;324(1):1-7. doi:10.1124/jpet.107.129031
65. Pacher P, Beckman JS, Liaudet L. Nitric oxide and peroxynitrite in health and disease. *Physiol Rev*. Jan 2007;87(1):315-424. doi:10.1152/physrev.00029.2006
66. De Miranda BR, Rocha EM, Castro SL, Greenamyre JT. Protection from alpha-Synuclein induced dopaminergic neurodegeneration by overexpression of the mitochondrial import receptor TOM20. *NPJ Parkinsons Dis*. Dec 8 2020;6(1):38. doi:10.1038/s41531-020-00139-6

67. Votyakova TV, Reynolds IJ. DeltaPsi(m)-Dependent and -independent production of reactive oxygen species by rat brain mitochondria. *J Neurochem*. Oct 2001;79(2):266-77. doi:10.1046/j.1471-4159.2001.00548.x
68. Ramsay RR, Singer TP. Relation of superoxide generation and lipid peroxidation to the inhibition of NADH-Q oxidoreductase by rotenone, piericidin A, and MPP+. *Biochem Biophys Res Commun*. Nov 30 1992;189(1):47-52. doi:10.1016/0006-291x(92)91523-s
69. Ibarra-Gutierrez MT, Serrano-Garcia N, Orozco-Ibarra M. Rotenone-Induced Model of Parkinson's Disease: Beyond Mitochondrial Complex I Inhibition. *Mol Neurobiol*. Apr 2023;60(4):1929-1948. doi:10.1007/s12035-022-03193-8
70. Eaton L, Welch I, Halal AK, Bengtsson J, Pamenter ME. Apocynin reduces dihydroethidium fluorescence in naked mole-rat cortex independently of NADPH oxidase. *Comp Biochem Physiol A Mol Integr Physiol*. Feb 2023;276:111342. doi:10.1016/j.cbpa.2022.111342
71. Moretti A, Ramirez A, Mink R. Xanthine oxidase does not contribute to apoptosis after brain hypoxia-ischemia in immature rabbits. *ISRN Neurosci*. 2013;2013:253093. doi:10.1155/2013/253093
72. Park TJ, Reznick J, Peterson BL, et al. Fructose-driven glycolysis supports anoxia resistance in the naked mole-rat. *Science*. Apr 21 2017;356(6335):307-311. doi:10.1126/science.aab3896
73. Russo E, Leoncini G, Esposito P, Garibotto G, Pontremoli R, Viazzi F. Fructose and Uric Acid: Major Mediators of Cardiovascular Disease Risk Starting at Pediatric Age. *Int J Mol Sci*. Jun 24 2020;21(12)doi:10.3390/ijms21124479
74. Ali SS, Hsiao M, Zhao HW, Dugan LL, Haddad GG, Zhou D. Hypoxia-adaptation involves mitochondrial metabolic depression and decreased ROS leakage. *PLoS One*. 2012;7(5):e36801. doi:10.1371/journal.pone.0036801
75. Buffenstein R, Yahav S. Is the naked mole-rat Hererocephalus glaber an endothermic yet poikilothermic mammal? *Journal of Thermal Biology*. 1991/07/01/ 1991;16(4):227-232. doi:https://doi.org/10.1016/0306-4565(91)90030-6
76. Saldmann F, Viltard M, Leroy C, Friedlander G. The Naked Mole Rat: A Unique Example of Positive Oxidative Stress. *Oxid Med Cell Longev*. 2019;2019:4502819. doi:10.1155/2019/4502819
77. Pamenter ME, Lau GY, Richards JG, Milsom WK. Naked mole rat brain mitochondria electron transport system flux and H(+) leak are reduced during acute hypoxia. *J Exp Biol*. Feb 20 2018;221(Pt 4)doi:10.1242/jeb.171397
78. Altenhofer S, Radermacher KA, Kleikers PW, Wingler K, Schmidt HH. Evolution of NADPH Oxidase Inhibitors: Selectivity and Mechanisms for Target Engagement. *Antioxid Redox Signal*. Aug 10 2015;23(5):406-27. doi:10.1089/ars.2013.5814
79. Chen R, Lai UH, Zhu L, Singh A, Ahmed M, Forsyth NR. Reactive Oxygen Species Formation in the Brain at Different Oxygen Levels: The Role of Hypoxia Inducible Factors. *Front Cell Dev Biol*. 2018;6:132. doi:10.3389/fcell.2018.00132
80. Nagel S, Genius J, Heiland S, Horstmann S, Gardner H, Wagner S. Diphenyleneiodonium and dimethylsulfoxide for treatment of reperfusion injury in cerebral ischemia of the rat. *Brain Res*. Feb 9 2007;1132(1):210-7. doi:10.1016/j.brainres.2006.11.023
81. Panday A, Sahoo MK, Osorio D, Batra S. NADPH oxidases: an overview from structure to innate immunity-associated pathologies. *Cell Mol Immunol*. Jan 2015;12(1):5-23. doi:10.1038/cmi.2014.89
82. Reis J, Massari M, Marchese S, et al. A closer look into NADPH oxidase inhibitors: Validation and insight into their mechanism of action. *Redox Biology*. 2020/05/01/ 2020;32:101466. doi:https://doi.org/10.1016/j.redox.2020.101466
83. Lambert AJ, Buckingham JA, Boysen HM, Brand MD. Diphenyleneiodonium acutely inhibits reactive oxygen species production by mitochondrial complex I during reverse, but not forward electron transport. *Biochim Biophys Acta*. May 2008;1777(5):397-403. doi:10.1016/j.bbabio.2008.03.005
84. Wang Q, Chu CH, Oyarzabal E, et al. Subpicomolar diphenyleneiodonium inhibits microglial NADPH oxidase with high specificity and shows great potential as a therapeutic agent for neurodegenerative diseases. *Glia*. Dec 2014;62(12):2034-43. doi:10.1002/glia.22724
85. Wind S, Beuerlein K, Eucker T, et al. Comparative pharmacology of chemically distinct NADPH oxidase inhibitors. *Br J Pharmacol*. Oct 2010;161(4):885-98. doi:10.1111/j.1476-5381.2010.00920.x